A NEW TEST METHOD TO CHARACTERIZE MIXED MODE II/III AND I/II/III DELAMINATION

Sang N. Nguyen[1], Carla Canturri Gispert[1], Emile S. Greenhalgh[1], Paul Robinson[1], Giuliano Allegri[1] and Kevin A. Brown[2]

[1] Imperial College, South Kensington, London, SW7 2AZ, UK, snguyen@imperial.ac.uk, www.imperial.ac.uk

[2] Rolls-Royce plc, C2, Moor Lane, Derby, DE24 8BJ, UK, kevinanthony.brown@rolls-royce.com, www.rolls-royce.com/

Keywords: Delamination, Toughness, Mixed Mode, Shear, Fractography

ABSTRACT

Delamination is a critical damage mechanism in laminated composites, and currently represents the greatest limitation to achieving lightweight damage tolerant designs of primary aircraft structures. Current mode III delamination toughness tests often generate additional damage processes other than mode III delamination, such as intralaminar ply splits and crack migration to neighbouring ply interfaces, which invalidate the toughness measurements. In this study, a test rig capable of generating mode II/III and I/II/III delaminations over a range of mode mixities, up to a threshold proportion of mode III, and almost uniform mode III strain energy release rates, has been designed, developed, trialled and validated. Preliminary mixed-mode tests have been conducted on Hexcel IM7/8552 with 0°/0° and 0°/90° ply interfaces at the delamination plane. Fractography has been performed to elucidate and understand the failure mechanisms and characterize the fracture morphologies associated with mixed-mode II/III and I/II/III delamination.

The fracture morphology of the IM7/8552 toughness coupons with a 0°/0° ply interface under pure mode II and mode II/III loading was exclusively delamination with little evidence of ply splitting or migration having had occurred. Directly ahead of the starter crack, the fracture morphology for both loading conditions presented a wedge of torn matrix, associated with the resin fillet. Beyond this fillet region, mode II/III loading presented slightly rotated cusps and a minor degree of fibre bridging. In summary, this paper presents a new mixed mode delamination test configuration, which still needs significant further development from the research community. In particular, the constraints applied to the specimen to achieve greater mode III components needs to be addressed. However, this new test method does offer a means to characterize delamination growth over a spectrum of mode-mixities which have not been achievable with existing test methods.

1 INTRODUCTION

The potential to make optimum use of laminated composites in primary aerostructures is often limited by the intrinsic critical vulnerability posed by the delamination. This weakness drives the need for excessive physical testing and is conceivably the greatest impediment to predictive modelling of progressive damage in composites. This research study was motivated by the dominance of mode III loading on the delamination processes in many primary composite aerostructures. The objective of the research was to develop a test method to characterize delamination fracture toughnesses over a range of mode II/III and I/II/III mixities up to a threshold proportion of mode III. Above this threshold, delamination has been observed to migrate to a different ply interface [1]. Characterization of the fractographic features generated under such conditions would be of great benefit in future failure investigations where a component of mode III loading may play a critical role in the governing failure process. The toughness data and the understanding of the delamination mechanisms gained through this research would interest developers of numerical models to more accurately capture delamination fracture processes in which migration could be a key feature. Such an understanding has the potential to greatly enhance the capability to develop more damage tolerant composite structures, which is critical

to realizing less conservative, more efficient structural design methodologies and perhaps accommodate progressive damage growth in future aerostructures. It should be stressed that the test method presented in this paper is not considered to be a complete and finalized method, but is currently a proposed (and demonstrated) concept, which needs to be refined and verified. The aim of this publication is to provide the opportunity for this concept to be considered by the wider research community and possibly developed collectively. The long-term goal is to achieve a configuration that can be accepted as an international standard mixed mode I/II/III delamination toughness test, as with the Mixed Mode Bend (MMB) test for mode I/II loading [2].

Currently, the most widely used approach to measure mode III delamination fracture toughness is to perform tests aiming to generate a uniform pure mode III strain energy release rate, G_{III}, along the crack front. In other words, the conventional starting point has been to develop a pure mode III test method, which could then be adapted to introduce additional mode I and mode II loading. For mode III, the Cracked Rail Shear (CRS) [3], variations of the Edge Crack Torsion (ECT) [4], the Modified Split Cantilever Beam (MSCB) [5] and the 4-Point Bending Plate (4PBP) [6] tests have been extensively studied. The major drawback of most mode III, mixed-mode II/III and I/II/III tests reported in the literature has been the development of ply splitting prior to delamination growth, which is thought to be common across all current test methods [7]. This implies that the apparent fracture toughness includes the energy required for the formation and propagation of these ply splits [8]. Furthermore, mode III and mixed-mode I/II/III test methods have often encountered difficulties in propagating a delamination at the intended ply interface. The delamination has been found to migrate to the neighbouring ply interfaces, especially in 0°/θ° ply interfaces (where 0° is the direction of global crack growth). Other common problems associated with these tests have been: the presence of non-linearity in the initial load-displacement response; the need for FE-based data reduction methods; difficulties in monitoring crack growth; non-uniform G distributions; the need to have large specimen areas; and a dependence on crack-length and specimen geometry. To achieve a large range of mode I/II/III mixities and closed-form data reduction methods, the Shear Torsion Bending (STB) rig has been developed, but this test requires edge delaminations and two independent loading actuators [9].

Previous research at Imperial College has demonstrated that for a given material, there is a threshold $G_{II/III}$ ratio which causes a delamination to migrate [10], and in such cases the delamination toughness cannot be characterized reliably. This implies that migration could be avoided if the mode III component is sufficiently small compared to the mode II component. The Width-Tapered End-Loaded Split (WTELS) test has been developed to measure this delamination migration threshold [1]. The aspiration of the present research was to formulate a new beam type test (akin to the MMB I/II test [2]) to generate a delamination having a controlled proportion of mode III. This has led to the development of two mixed-mode delamination tests for characterizing mode II/III and I/II/III mixities, namely the Mixed Mode Shear (MMS) and Mixed Mode Opening (MMO) tests (Figures 1 and 2), respectively, which use a beam specimen, akin to the Double Cantilever Beam (DCB) specimen. Numerical modelling of these tests using the Virtual Crack Closure Technique (VCCT) [11] in Abaqus 6.14-1 [12] has demonstrated that they generate an almost uniform G_{III} along the crack front. This modelling has been used to determine the different loading configurations required in the tests to achieve a given mode-mixity and to calculate the toughness values using experimentally determined initiation failure loads. In summary, the novel test method developed in this research originated from a standard mode II loading configuration, and inclining the beam specimen about its longitudinal axis to introduce increasing proportions of mode III loading, with or without mode I loading. A large range of I/II/III mode mixities can be achieved with the use of a single loading actuator and small specimens, which makes this test more economical for widespread use and amenable to standardization compared to tests requiring relatively large plates [6] or two independent actuators [9].

2 MIXED MODE SHEAR/OPENING TEST METHODS

This experimental Section describes the panel and specimen manufacture, test procedure and test matrix for the delamination toughness tests. Two configurations of the test were developed: a mixed mode II/III condition (MMS), in which the test specimen was loaded with a compressive mode I component (Figure 1) and a mixed mode I/II/III condition (MMO), in which the other arm of the test

specimen was loaded in the same direction to give an opening mode I component (Figure 2). In simplistic terms, the former was a superposition of the pure mode II End Loaded Split (ELS) and pure mode III MSCB tests, whilst the latter was a superposition of the mixed-mode I/II [2] and the pure mode III MSCB tests. For both test methods, the specimen dimensions were identical. The mode-mixity at the inclination angle shown in Figure 1 was $G_{II}/G_T = 35\%$ and $G_{III}/G_T = 1.5\%$. The low value of G_{III}/G_T was a consequence of the unloaded arm having no lateral constraint at the free end. To achieve greater G_{III}/G_T ratios, the test rig needs to be revised by, for instance, introducing an additional constraint to the free end of the unloaded arm, such that it cannot follow the lateral motion of the upper arm.

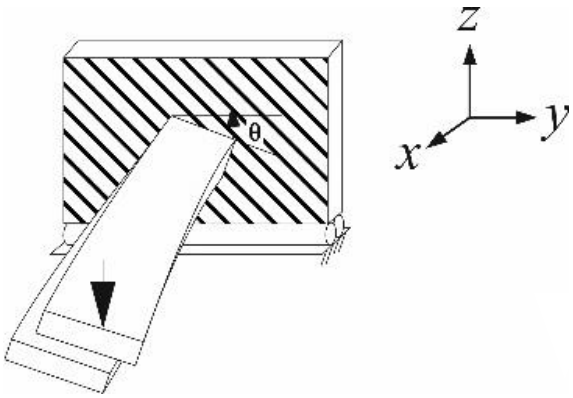

Figure 1: Schematic of mode II/III (MMS) test configuration

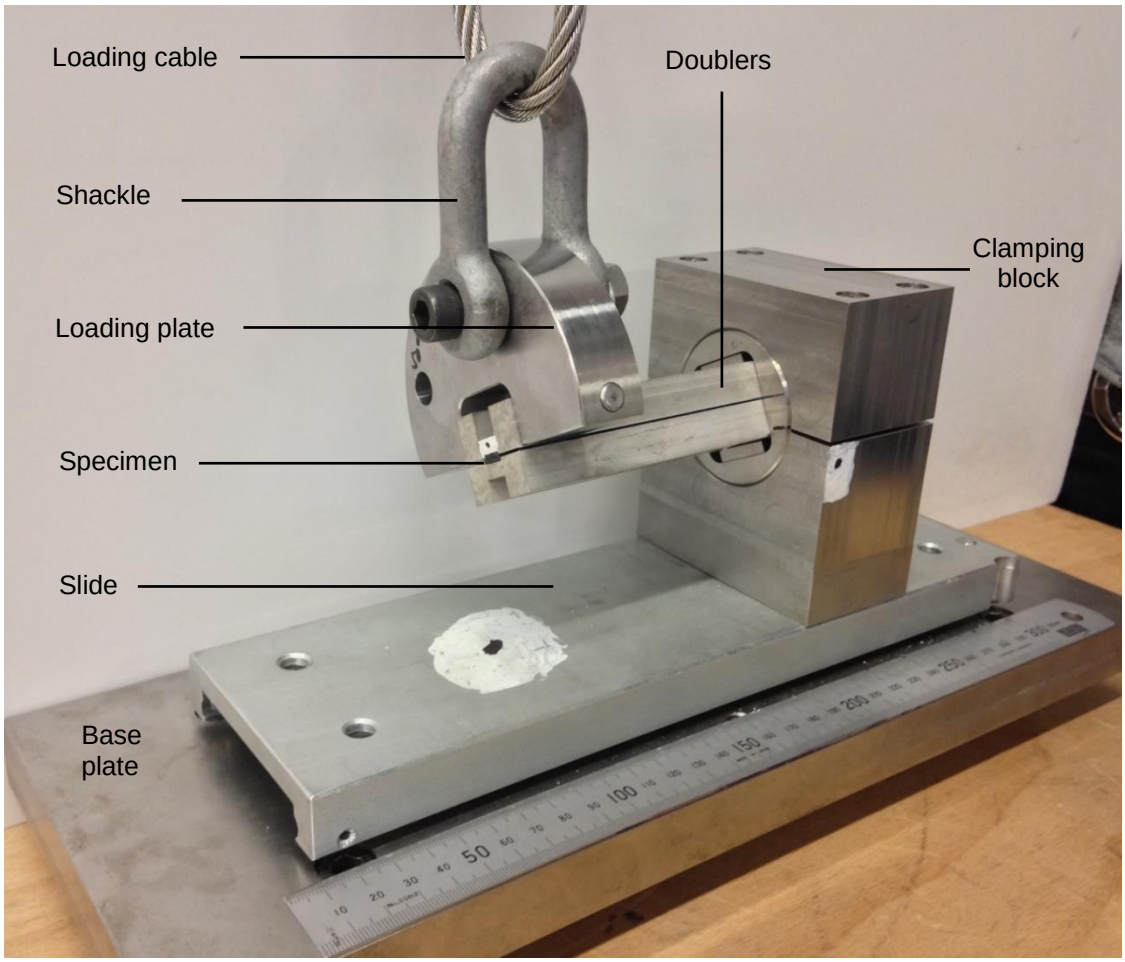

Figure 2: Mixed mode opening (MMO) fixture

2.1 Specimen manufacture

Hexply IM7/8552 (33% UD 134 12K [13]) test specimens were hand laid-up and cured following the supplier's recommended cure schedule in an LBBC Quicklock autoclave. The stacking sequences for the panels were $(0/90)_{3s}//(0/90)_{3s}$ for the 0°/0° mid-plane ply interface panel and $(0/90)_{3s}//(90/0)(0/90)_2/(90/0)_3$ for the 0°/90° mid-plane ply interface panel. A 10 μm PTFE film acting as a starter crack was inserted at the laminate mid-plane during the layup and the specimens were cut using a dry diamond saw. The panels had dimensions of 300 mm × 200 mm, allowing a maximum of twenty-four 155 mm × 10 mm × 3 mm specimens to be cut from each panel. The panels were C-scanned in an immersion tank both after the cure and after cutting to verify there had been no manufacturing defects or finishing damage. An ultrasonic 10 MHz focused probe with a 50 mm focal distance was used in Time of Flight (TOF) mode and coupled to a full waveform capture system (VisualScan by Tecnitest).

The panel edges were trimmed such that the edge of the loaded end was 72.5 mm from the tip of the starter crack. The clamped end was then trimmed such that all specimens had a total length of 155 mm. During the test development, doublers [14] were designed to ensure the test piece arms were stiff enough to impart the required strain energy to cause delamination rather than flexural failure. Refinement of this design was required to ensure plastic deformation of the doublers at the load introduction point was eliminated. The refinement of the loaded doublers was identical to the unloaded doublers, with the exception that the loaded doublers had an additional 2 mm thickness over a 25 mm length above the loading hole to prevent yielding at this hole. The doublers were fabricated from aluminium 7075 T651 to ensure sufficient strength, and the surfaces to be bonded to the composite specimen were grit blasted and acid etched prior to bonding.

2.2 Test rig development

During test development, it was recognized that deflection and twisting of the specimen out of the plane of the test rig could introduce lateral loads onto the load cell. To minimize this effect and reduce over-constraint, a long load-train was used, with a 1 m long, 8 mm diameter steel cable used to transmit load to the specimen (Figure 2). This cable was housed within (but isolated from) a PVC pipe to protect against any potential cable failures. For pure mode II tests, the cable was not needed, and so was not used to keep the rig compliance as low as possible. For tests involving some mode III component, the cable was used to allow a lateral degree of freedom and rotation about the vertical axis. The mixed mode opening test setup (Figure 2) allows the introduction of mode I loading (in addition to modes II and III). This opening component was postulated to avoid any high frictional forces which would damage the fracture surfaces, and hence manifest as enhancements in toughnesses. The hole locations were chosen to ensure that the load line passed directly through the specimen shear centre. For both the MMS and MMO test rigs, two separate loading plates were required to enable holes at 10° intervals to be machined without any overlapping of the holes in the plates.

2.3 Experimental procedure

The specimens were tested in an Instron 5969 universal testing machine, equipped with a 50 kN load cell. The rig base plate was bolted onto the base of the test machine and the upper end of the steel cable was gripped centrally within the jaws attached to the upper crosshead. The cable and loading plate were connected to the loaded end of the specimen using the loading rod and shackle, and the specimen was bolted into the cylindrical specimen holder. The specimen inclination angle was adjusted to give the desired mode-mixity, and a check was made to ensure the intended loading hole was directly above the specimen centerline. The required inclination from the horizontal (θ) of the loading plate to achieve known mode-mixities was determined from numerical modelling. The shackle was then bolted through the loading hole in one doubler and the cylindrical specimen holder was then secured via the clamping block bolts. Clear high-contrast markers were placed at the loaded end and the clamped end. An Imetrum optical strain system was used measure the displacement of the pin at the loaded end relative to the clamping block at a sampling rate of 10 Hz. The crosshead speed was chosen to a give a displacement rate at the loaded end of approximately 1 mm/min. Once the specimen had failed, the load was returned to zero and the specimen was removed by unbolting the shackle and unclamping the support block. The

doublers were checked for any signs of yielding by placing them on a flat surface and ensuring they had remained straight. If this was not the case, the test was deemed invalid.

2.4 Summary of test parameters

Three delamination (mode-mixity) conditions were investigated: pure mode II ($\theta = 0°$), mixed mode II/III ($G_{III}/G_T = 10\%$, $\theta = 30°$) and mixed mode I/II/III ($G_I/G_T = 63.5\%$, $G_{III}/G_T = 1.5\%$, $\theta = 30°$), where θ was the specimen inclination from the horizontal about the longitudinal axis. The pure mode II tests enabled comparison with toughness values reported in the literature. The delamination resistance of two ply interfaces (0°/0° and 0°/90°) were characterized. For each test configuration, at least five valid tests were undertaken, except in one case where only four specimens could be obtained from the panel, since some specimens had been used for preliminary trials. All 0°/90° specimens were tested such that the 0° ply at a 0°/90° ply interface would be on the tension face to reduce the likelihood of migration [1]. Only the initiation toughness was measured, since the crack growth was unstable. In the test development, the starter crack length was large and the crack tip was close to the clamp, since the aim was to generate stable growth, as predicted by numerical modelling. However, the tests produced unstable crack growth, leading to the difficulties discussed later in this paper.

3 NUMERICAL ANALYSIS

Since the experimental data analysis required an FE based data reduction method, this Section describes the modelling strategy used for the calculation of the delamination fracture toughness. To refine the test rig and determine the rig configuration and loading plate inclination to generate known mode-mixities, the specimens were modelled using Abaqus CAE 6.14-1 (Figure 3). The specimens were modelled with six layers of C3D8R solid elements with one reduced integration point per ply and the constitutive properties listed in Table 1. The delaminated region behind the starter crack front was modelled by leaving those nodes untied. Frictionless contact constraints were added at the surface representing the insert to avoid interpenetration. Boundary conditions were applied as prescribed displacements directly at the nodes of the doublers along the line where the loading pin would pass through the reinforced doubler hole.

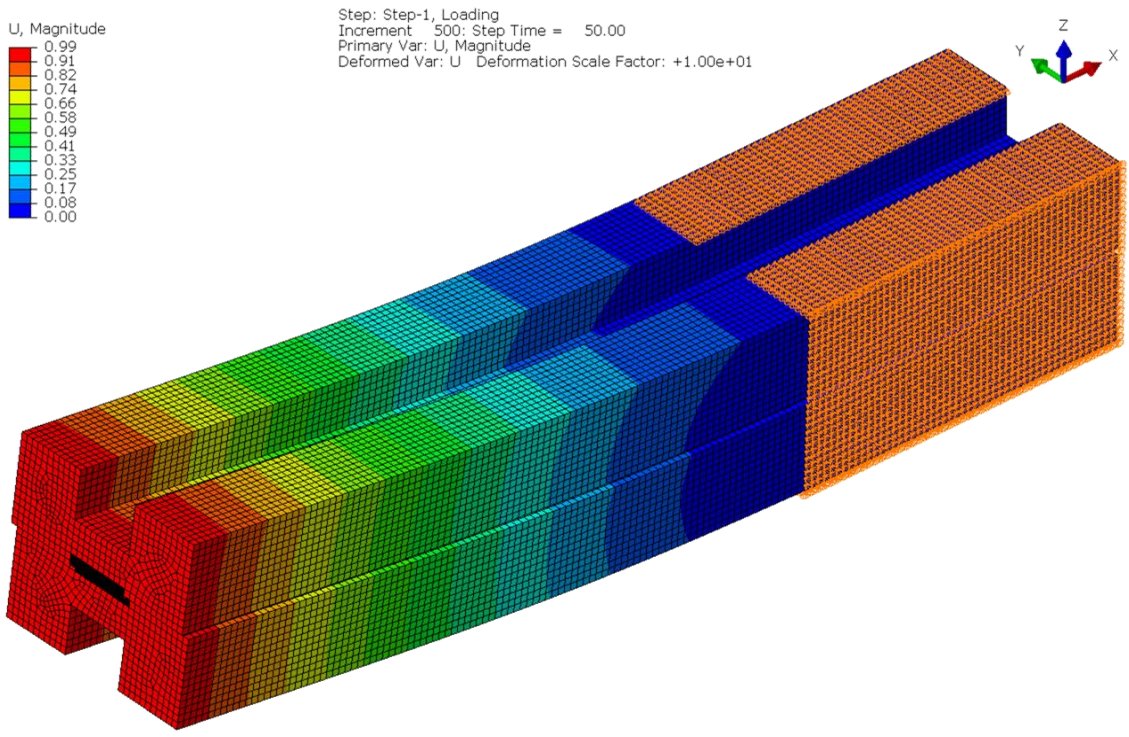

Figure 3: Mesh and boundary conditions for the numerical model of a 150 mm long MMS specimen

Material	E_{11}	E_{22}	E_{33}	G_{12}	G_{13}	G_{23}	ν_{12}	ν_{13}	ν_{23}
IM7/8552 [15]	165	9.4	10.5	4.50	4.29	3.19	0.30	0.31	0.49
Al 7075-T651 [16]	72.8	72.8	72.8	27.9	27.9	27.9	0.33	0.33	0.33

Table 1: Elastic properties used in the numerical models (all moduli have units of GPa)

The VCCT in ABAQUS was used to determine the strain energy release rates at the crack front. The clamping was modelled as a fully clamped support and the adhesive between the doublers and the specimen was modelled as a tied surface constraint. The numerical analysis here focused only on modelling the specimen and doublers to enable a finer mesh for these parts. The deformed mesh of the doublers and the specimen is shown in Figure 3 and the strain energy release rate (SERR) distributions along the crack front are shown in Figure 4.

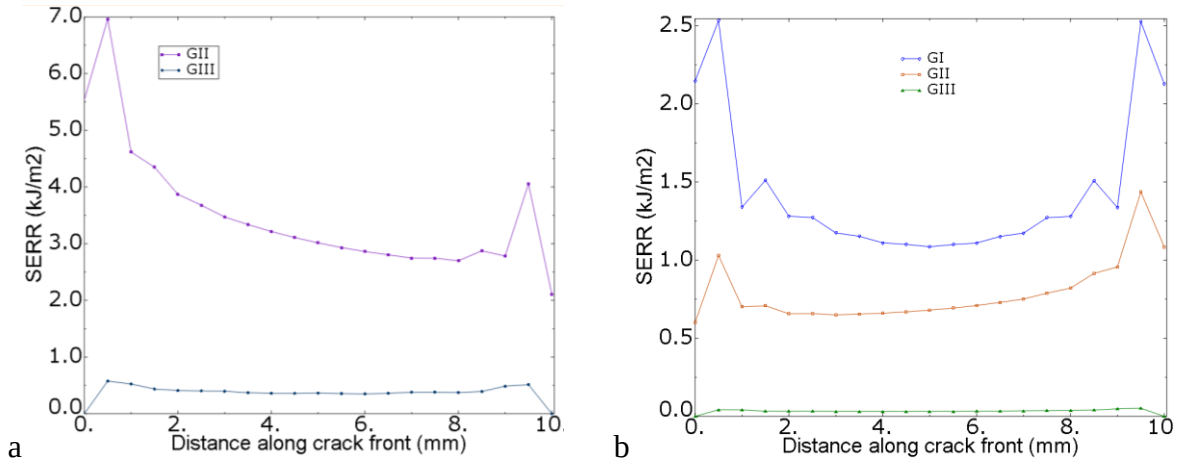

Figure 4: SERR distributions along the crack front for (a) mode II/III and (b) mode I/II/III

The model for the pure mode II test allowed one translational degree of freedom. However, for the mixed mode tests (Figures 1 and 2), it was necessary to introduce a lateral translational degree of freedom to prevent a lateral force on the load cell during the test, as the specimen would bend about the vertical axis as well as about the horizontal. The loading was modelled as a prescribed upward displacement of 1 mm applied along a line of nodes 12.5 mm from the free end of the doublers over a time of 60 to 90 s. For mode II or II/III loading (MMS), the lower doubler was displaced and for mode I/II/III (MMO), the equivalent nodes on the upper doubler were displaced. At these loaded nodes, the longitudinal (x) displacement was constrained to be zero and the clamped end was free to translate in the x direction. The clamped length of the model was updated to match that in the fixture of 50 mm. Over the clamped length at the upper and lower surfaces of the upper and lower doublers respectively, the vertical (z) displacement was constrained to be zero. Along one side of both doublers, over the clamped length, the lateral (y) displacement was zero. Finally, all rotational degrees of freedom remained unconstrained. Models involving mode III configurations were generated by taking the pure mode II models and rotating the whole specimen assembly about the longitudinal (x) axis by a specified angle and keeping all other conditions unchanged.

4 RESULTS AND FRACTOGRAPHIC OBSERVATIONS

The load-displacement curves (Figure 5) presented a sharp load drop at delamination initiation and the test was unstable. In some cases, particularly for the mode II/III tests, there was no load drop observed and these invalid tests was stopped before a load could be reached which could cause yielding of the doublers. In general, the load did not drop fully to zero, but once it reduced, the load continued to rise again following a different stiffness response.

The critical strain energy release rates were calculated by using the ultimate loads from the tests normalized to a specimen width of 10 mm, as this was the width used in the models. For each specimen,

the ultimate load was multiplied by 10/*b*, where *b* is the specimen width in mm. From the numerical models (run for durations such that the loads exceeded the test ultimate loads), the relationship between the average strain energy release rate (G^a) across the crack front and square of the load (P^2) was determined and therefore the term G^a/P^2 could be deduced from the models. The square of the normalized initiation failure load, P^{*2}, from the tests was multiplied by G^a/P^2 to determine an effective G_c, A summary of the average initiation delamination toughnesses for IM7/8552 specimens with 0°/0° and 0°/90° mid-plane ply interfaces is presented in Table 2.

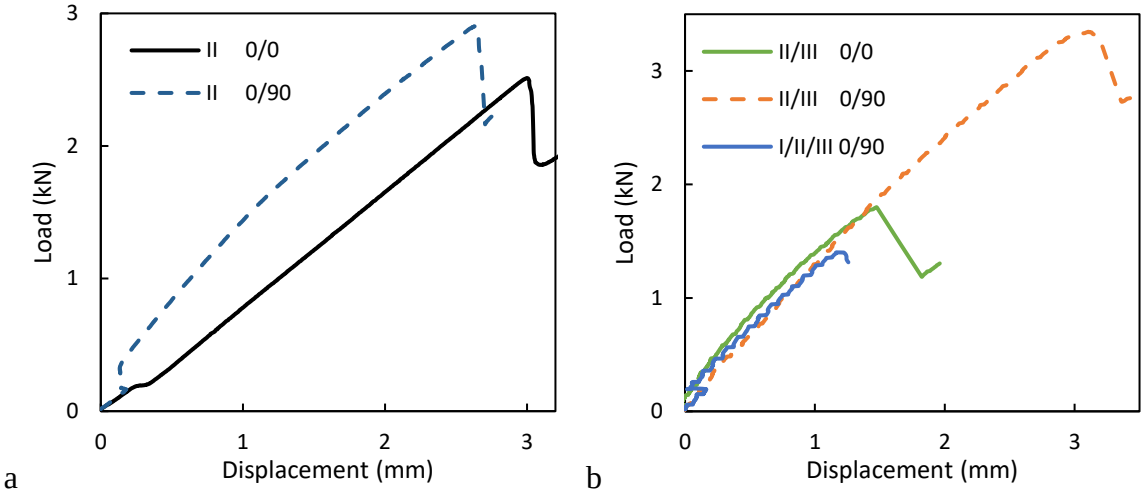

a b

Figure 5: Typical load displacement curves for (a) pure mode II and (b) mixed mode II/III and I/II/III

Ply interface	Mode	G_I/G_T (%)	G_{II}/G_T (%)	G_{III}/G_T (%)	G_{TC} (kJ/m^2)	CV (%)
0°/0°	II	0	100	0	1.23	28
0°/0°	II/III	0	90	10	0.61	21
0°/90°	II	0	100	0	1.21	45
0°/90°	II/III	0	90	10	2.29	10
0°/90°	I/II/III	64	35	1.5	0.85	28

Table 2: Summary of initiation delamination fracture toughnesses for IM7/8552

The fracture surfaces were examined to find evidence of the mode-mixity and friction between the surfaces caused by any compressive mode I loading. To examine the fracture surfaces, the delaminated plies were exposed by inserting a chisel at the delamination plane and inducing a pure mode I delamination (without contacting the original delamination surface). The sub-laminates were removed from the doublers in the same way, taking care to minimise any post-failure damage. In some specimens, any fibers bridging between the sub-laminates were cut to aid separation of the surfaces. The specimens were mounted on stubs and gold sputtered for 20 s in an Agar Automatic sputter coater. Silver paint was applied over the corners of the specimen and around the edges of the stubs. A Hitachi S-3700N scanning electron microscope at magnifications of ×50, ×100, ×500 and ×1000 with an acceleration voltage of 10-15 kV was used for detailed fractographic analysis of both uppermost and lowermost failure surfaces.

The approach undertaken was to first identify three specimens from each identical test configuration that could represent the full range of fracture morphologies present under the associated test conditions. Micrographs close to the crack tip, at the centre, followed by the left and right edges were captured to understand the effect of the position across the specimen width on the morphology. The micrographs

focussed on any evidence of migration and the twisting of the cusps that would indicate the presence and severity of mode III delamination. To understand how the delamination conditions changed as the crack propagated, micrographs were also captured at 6 mm and 12 mm distances from the crack tip along the centreline and along the left and right edges on the uppermost surface. The micrographs were taken at 0˚ tilt unless otherwise specified.

The fractographic examination presented here focussed primarily on the specimens with 0°/0° ply interfaces and delaminations directly adjacent to the starter crack. This was because the delamination growth was unstable and therefore no toughness data could be obtained that were associated with the surfaces away from the insert tip. Only a brief analysis of the 0°/90° ply interfaces was carried out because migration was found to be prevalent for this ply interface under all loading conditions, and therefore the corresponding toughness values could not be considered as valid measurements of the toughness of the intended ply interface.

Under both delamination conditions for the 0°/0° ply interfaces, the fracture surfaces (Figure 6) were dull with a whitish appearance and there was no evidence of tide marks on the surfaces. The fracture morphology at low magnification just ahead of the starter crack, at the mid-width of each specimen, is shown in Figure 7. The presence of the PTFE insert in this region had led to a thickening of the resin at the interply region, producing a 'resin fillet' ahead of this starter crack. This region was the site over which the toughness was measured. Directly ahead of the starter crack, the fracture morphology for both loading conditions presented a wedge of torn matrix, associated with the resin fillet. Beyond this, both loading conditions presented cusps and a minor degree of fiber bridging. The fracture morphology at high magnification just ahead of the starter crack, at the mid-width of the mode II/III specimen is shown in Figure 8 (note that mode I/II/III was not tested for the 0°/0° ply interface). For both loading conditions, the failure mode was exclusively delamination, although there was evidence of fiber bridging having developed.

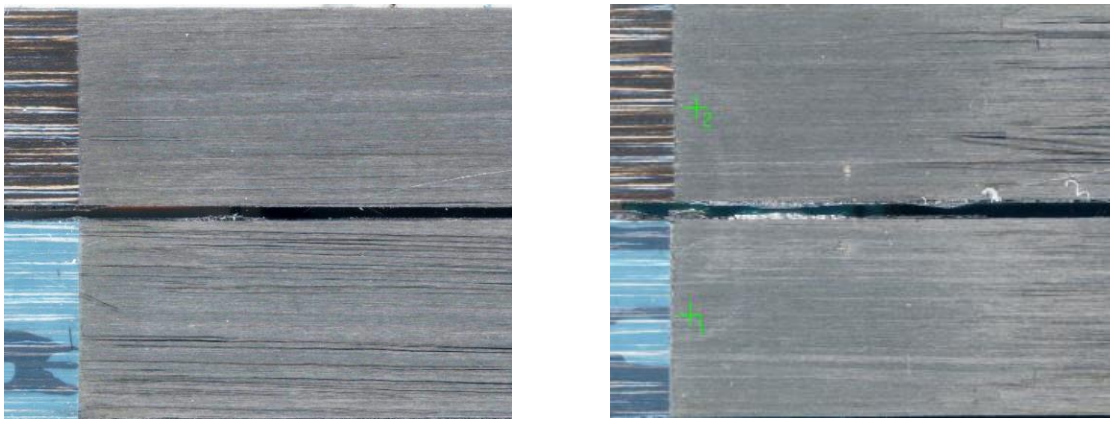

(a) Pure mode II (b) Mode II/III

Figure 6: Flatbed scans of the fracture morphology for 10 mm wide 0°/0° interface specimens

The fracture morphologies associated with a 0°/90° ply interface under pure mode II, mode II/III and mode I/II/III loading close to the starter crack (Figure 9) all presented some evidence of off-axis ply splitting and/or migration, which would manifest as enhanced toughness. This illustrated that the fracture plane was a combination of splitting of the 90° plies and cohesive delamination fracture at the original defect plane for all three loading conditions. For the pure mode II condition, there was some minor splitting which had developed from one edge, but most of the surface was consistent with the original defect plane. However, for the mode II/III and mode I/II/III delamination surfaces, significant splitting had developed.

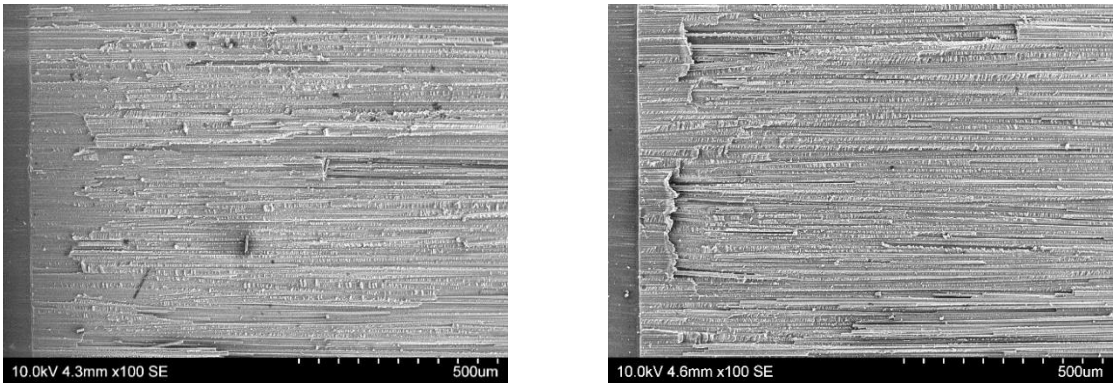

(a) Pure mode II

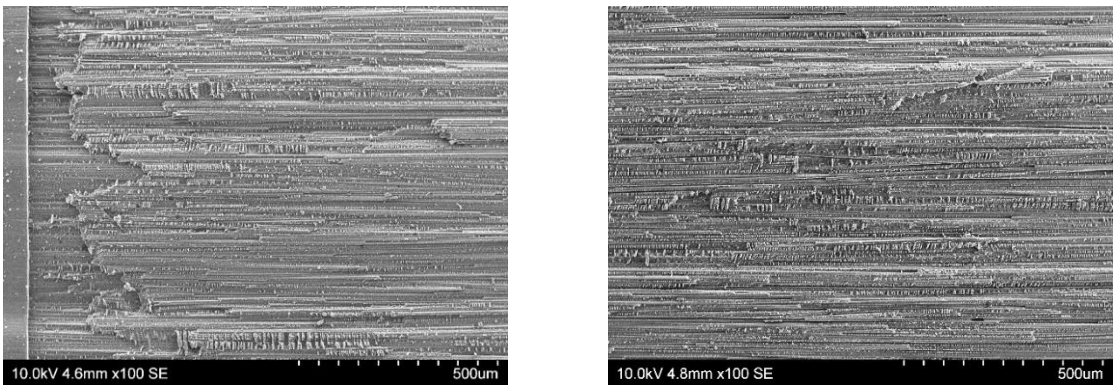

(b) Mode II/III

Figure 7: Fracture morphology for IM7/8552, 0°/0° ply interface showing the lowermost surface (left image) and uppermost surface (right image) at the mid-width, close to the starter crack, ×100

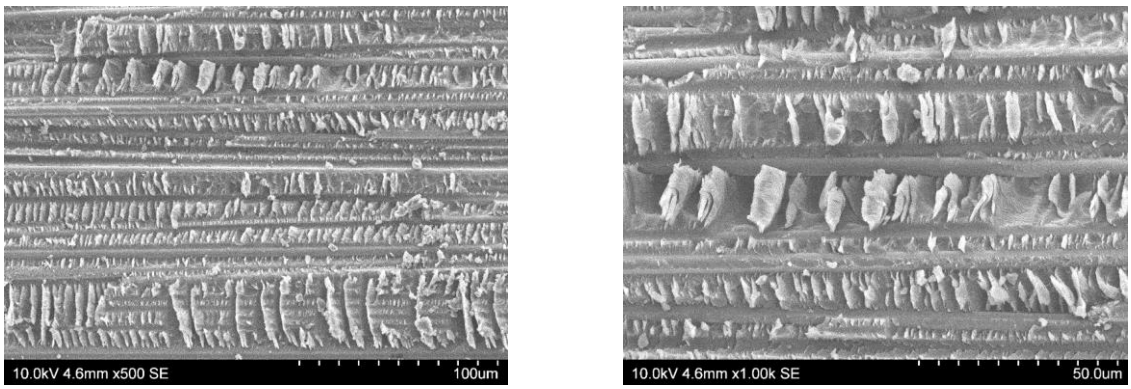

×500 ×1000

Figure 8: Fracture morphology for IM7/8552, 0°/0° ply interface at the mid-width, close to the starter crack under mode II/III loading.

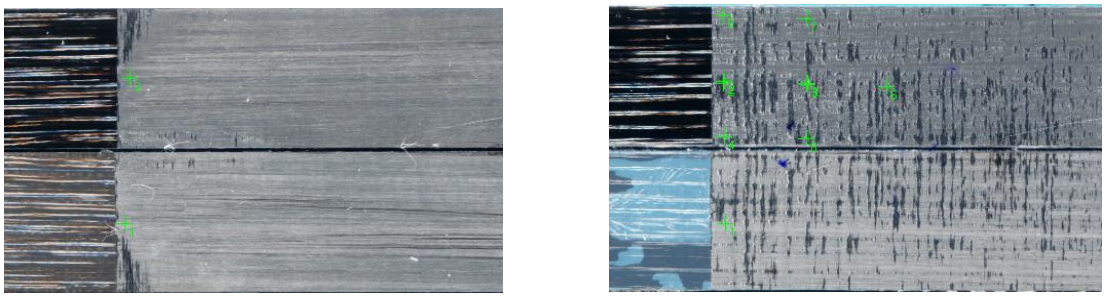

(a) Pure mode II (b) Mode II/III

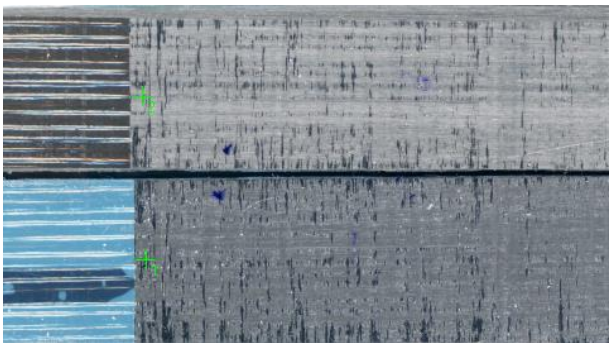

(c) Mode I/II/III

Figure 9: Flatbed scans of the fracture morphology for 10 mm wide 0°/90° ply interface specimens

6 DISCUSSION

The MMS and MMO test methods developed through this research were successful in determining mixed-mode II/III and I/II/III delamination toughnesses and generating valid fracture morphologies for 0°/0° ply interfaces. There remain, however, questions over the 0°/90° interface toughnesses, because the fracture surfaces presented evidence of 90° splitting. The test itself was relatively straightforward to perform and the specimens were economical in material usage as compared to other mode III plate methods, such as the modified ECT [4] and the 4PBP [6] tests. Due to the presence of the aluminum doublers, the G_{III} distribution was almost uniform across the crack front. However, detailed analysis of the critical strain energy release rates suggested that there had been coupling between the mode II and the mode III loading components, especially near the edges of the specimen width. In its current form, there are however several issues with the test rig and specimen manufacture that led to variability in the toughness values and lower mode III components for a given inclination angle than desired. These issues are discussed in the following sub-Sections.

6.1 Through-thickness compression and friction

In the case of pure mode II and mode II/III loading, the high stiffness of the specimen (i.e. CFRP plus doublers) in the direction perpendicular to the plane of the laminate resulted in greater compressive mode I components than would be the case for a specimen having no doublers. This high friction between the sub-laminates promoted wear between the fracture surfaces, making it more difficult to observe the resulting fractographic features. In addition, this crushing expended energy and therefore inflated the apparent toughness measurements. The proposed method to remedy this problem was to load the upper arm upwards, thus introducing an opening mode I component. However, this mode I component was inversely related to the mode III component, as tilting the specimen to greater inclination angles would have reduced the mode I component. An alternative approach to prevent high through-thickness compressive stresses arising, whilst still loading the lower arm, would be to wedge a small roller [17] or bearings in between the arms of the specimens, in such a way that the mode II and mode III degrees of freedom would not be affected.

6.2 Boundary conditions

The proximity of the starter crack tip to the clamp was considered to have had a significant influence on the variability of the results. In these tests, the current distance between the crack front and the face of the clamp was only 29 mm. The original starter crack length was selected to be greater than 55% of the free length to increase the propensity of a stable crack growth, as in the ELS test. However, since unstable crack growth occurred nevertheless, this condition was not sufficient and the scope of data reduction was restricted to determination of the initiation toughness only. Future tests will therefore reduce the initial crack length so that the boundary conditions at the clamped end would have a smaller influence on the loading conditions at the crack tip.

A current limitation, which particularly applied to the mode I/II/III test configuration, was that the free end of the unloaded arm of the specimen was not constrained against lateral motion relative to the loaded arm. Thus, the unloaded arm would effectively be pulled in the same lateral direction as the loaded arm, and so the mode III component was much lower than would have been the case if the loaded arm was constrained. To achieve greater mode III components for the same inclination angle, a roller support could be added such that only out-of-plane bending and not in-plane bending of the unloaded arm could take place. The roller support would need to change angle with the inclination of the specimen to ensure the constraint would always act in the correct direction.

6.5 Delamination toughnesses

Compared to reference values of G_{IIC} for IM7/8552 of 0.61 kJ/m^2 [15] and approximately 1.30 kJ/m^2 [18], the 0°/0° interface toughness measured here of 1.23 kJ/m^2 fell within the upper part of this large range. The large inherent variability in the fracture toughness values obtained using the current test method were attributed to two mechanisms observed during fractography. The first was that there was evidence that the fracture processes had been influenced by the thickened resin region directly ahead of the starter crack, which was attributed to the specimens not having a pre-crack in this study. Pre-cracking is used in the mode I [19] and mode II standards [17], whilst the use of metal shims has been found to produce fracture toughnesses which have better reproducibility than those generated using PTFE inserts [18]. The second observation was the crushing of the fracture surfaces at the uppermost edge of the specimens loaded under mode II or mode II/III. Post-fracture deformation of the surfaces would have increased the apparent measured toughness and the lower toughness of the mode I/II/III loaded specimens would support this premise.

The next steps in this research will involve refining the test method and further characterizing the mixed-mode II/III and I/II/III fracture toughnesses for IM7/8552 focusing on 0°/0° mid-plane ply interfaces. Pre-cracking of the specimens will be used so that the initial starter crack will extend beyond the resin fillet region. Shorter starter crack lengths will also be used to reduce the influence of the clamping conditions on the initiation toughness. A further refinement of the test will investigate improving the repeatability of the specimen manufacturing process and reducing the frictional effects that can degrade the fracture surfaces.

6 CONCLUSIONS

In summary, this research has successfully developed unique Mixed Mode Shear (MMS) and Mixed Mode Opening (MMO) beam type initiation delamination fracture toughness test methods based on a superposition of established pure mode tests. The test rig can generate mode II/III and I/II/III delaminations with a large range of mode mixities and almost uniform mode III SERRs. The mixed mode tests conducted have generated fracture surfaces under controlled conditions using IM7/8552 specimens with both 0°/0° and a 0°/90° mid-plane ply interfaces. The key conclusions and findings pertinent to attaining more reliable and accurate mixed mode delamination toughness measurements are:

- The test rig and data reduction method (currently via FE modelling) needs further development to become a test standard.
- The presence of a mode III component causes the cusps to be twisted about a plane perpendicular to the laminate to a degree governed by the relative proportion of mode III.
- Pre-cracking should be used to extend the crack tip beyond the resin fillet region and the starter crack length should leave a larger distance between the pre-crack and the clamp face.
- Under mode II/III loading, the fracture surfaces experience compressive stresses that can lead to crushing of the surfaces thereby increasing the apparent toughness.
- The toughnesses for the 0°/90° ply interface specimens could not be considered valid due to their susceptibility to ply splitting and delamination migration as witnessed in the fractographs.

ACKNOWLEDGEMENTS

The authors would like to acknowledge support provided by Rolls Royce under the SILOET2 programme and thank Dr Rodolfo Rito for his assistance in acid etching of the doublers. Appreciation

is also expressed to Roland Hutchins, Gary Senior, Jon Cole, Joseph Meggyesi, Keith Wolstenholme and Frank Gommer for their technical support and assistance with the manufacturing of the specimens and test fixture throughout the project.

REFERENCES

[1] C. Canturri Gispert, E.S. Greenhalgh and S.T. Pinho, The relationship between mixed-mode II/III delamination and delamination migration in composite laminates, *Composites Science and Technology*, **105**, 2014, pp. 102–109.

[2] ASTM D6671/D6671M-13e1 Standard test method for mixed mode I-mode II interlaminar fracture toughness of unidirectional fiber reinforced polymer matrix composites, *ASTM International*, West Conshohocken, PA, 2013.

[3] G. Becht, J.W. Gillespie, Design and Analysis of the Crack Rail Shear Specimen for Mode-III Interlaminar Fracture, *Composites Science and Technology*, **31**, (2), 1988, pp. 143-157.

[4] J M.W. Czabaj, B.D. Davidson and J.G. Ratcliffe, A modified edge crack torsion test for measurement of mode III fracture toughness of laminated tape composites, *NASA Technical Paper*, **1706**, 2016.

[5] P. Robinson and D.Q. Song, The development of an improved mode-III delamination test for composites. *Composites Science and Technology*, **52**, (2), 1994, pp. 217-233.

[6] A.B. de Morais, A.B. Pereira, Mode III interlaminar fracture of carbon/epoxy laminates using a four-point bending plate test. *Composites Part A: Applied Science and Manufacturing*, **40**, (11), 2009, pp. 1741-1746.

[7] A.L. Johnston and B.D. Davidson, Intrinsic coupling of near-tip matrix crack formation to mode III delamination advance in laminated polymeric matrix composites. *International Journal of Solids and Structures*, **51**, 2014, pp. 2360-2369.

[8] M.W. Czabaj, J.G. Ratcliffe and B.D. Davidson, Observation of intralaminar cracking in the edge crack torsion specimen. NASA Technical Publication 2013, 218143.

[9] B.D. Davidson, F.O. Sediles. Mixed-mode I–II–III delamination toughness determination via a shear–torsion-bending test. *Composites Part A: Applied Science and Manufacturing*, **42**, (6), 2011, pp. 589-603.

[10] C. Canturri, E.S. Greenhalgh, S.T. Pinho and J. Ankersen, Delamination growth directionality and the subsequent migration processes – the key to damage tolerant design. *Composites Part A: Applied Science and Manufacturing*, **54**, 2013, pp. 79-87.

[11] R. Krueger, The virtual crack closure technique for modelling interlaminar failure and delamination in advanced composite materials, *Numerical modelling of failure in advanced composite materials*, Woodhead Publishing, 2015, pp. 3–53.

[12] Dassault Systèmes, Simulia, Abaqus CAE v6.14-1, 2015 (CR-1974).

[13] Hexcel Corporation, HexPly® 8552 curing epoxy matrix product datasheet, FTA 072e, 2013. http://www.hexcel.com/Resources/DataSheets/Prepreg-Data-Sheets/8552_eu.pdf

[14] J.R. Reeder, K. Demarco and K.S. Whitley, The use of doublers in delamination toughness testing, *Composites Part A: Applied Science and Manufacturing*, **35**, (11), 2004, pp. 1337-1344.

[15] CASA/SAAB EDAVCOS, IM7/8552 Material properties, 1999.

[16] Granta Design, *Cambridge Engineering Selector EduPack*, 2016.

[17] ASTM D7905/D7905M-14, Standard test method for determination of the mode II interlaminar fracture toughness of unidirectional fiber-reinforced polymer matrix composites, 2014.

[18] Y.M.L. Cahain, J. Noden and S.R. Hallett, Effect of insert material on artificial delamination performance in composite laminates, *Journal of Composite Materials*, **49**, 2015, pp. 2589–2597.

[19] ASTM D5528-13, Standard test method for mode I interlaminar fracture toughness of unidirectional fiber-reinforced polymer matrix composites, 2013.